INSTITUTE OF PHYSICS PUBLISHING JOURNAL OF PHYSICS A: MATHEMATICAL AND GENERAL

J. Phys. A: Math. Gen. **36** (2003) 5773–5786 PII: S0305-4470(03)58242-7

Generalized coherent states for the double-well potential

M Novaes[1], **M A M de Aguiar**[2] **and J E M Hornos**[1]

[1] Instituto de Física de São Carlos, Universidade de São Paulo, CP 369, 13560-970, São Carlos, SP, Brazil
[2] Instituto de Física 'Gleb Wataghin', Universidade Estadual de Campinas, 83-970, Campinas, SP, Brazil

E-mail: marcel@if.sc.usp.br

Received 13 January 2003, in final form 1 April 2003
Published 13 May 2003
Online at stacks.iop.org/JPhysA/36/5773

Abstract

We construct generalized coherent states for the one-dimensional double-well potential and calculate their Mandel parameter, uncertainty relation and Wigner functions. The singularities of their autocorrelation function undergo bifurcations as the mean energy of the system is varied, and we analyse their structure. In the high-energy regime these states consist of a coherent superposition of two minimum-uncertainty Gaussians (they are Schrödinger catlike states).

PACS numbers: 42.50.Ar, 03.65.Ud

1. Introduction

The coherent states of the harmonic oscillator

$$|\alpha\rangle = \mathrm{e}^{-|\alpha|^2/2} \sum_{n=0}^{\infty} \frac{\alpha^n}{\sqrt{n!}} |n\rangle \tag{1}$$

have a series of remarkable properties, namely they are eigenstates of the annihilation operator, are obtained from vacuum by a displacement operator, minimize the Heisemberg uncertainty relation and are overcomplete. All these properties have served as guidelines for different generalizations: the first and the second ones rely on some kind of algebraic structure behind the system in question [1], while the last two are more general [2].

In this paper we consider the application to the double-well potential of a recent proposal of generalized coherent states [3], the Gazeau–Klauder (GK) states, which appears to be the most general one, imposing only normalizability, continuity on the parameter and completeness (also called resolution of the identity). Besides these basic demands, when dealing with physical

systems one often requires temporal stability, meaning that the time evolution of a coherent state is another coherent state.

These states were constructed recently for the one-dimensional Poschl–Teller oscillator (the infinite square well being a limiting case) [4], where the presence of exact solutions in analytic form allows a complete analysis of the problem. Other examples are the nonlinear oscillators that appear in [5] and the calculation presented in [6] for a periodic potential, where the GK states are compared to the canonical coherent states. The relation between these states and generalized uncertainty relations was explored in [7], and a suitable Moyal bracket was constructed in [8]. An extension of the GK states for higher dimension was made in [9], where the formalism was applied to a two-dimensional thermodynamical problem.

The double-well potential has attracted some attention over the years because of its similarity to the $\phi^2 + \lambda\phi^4$ quantum field theory, which is the prototype of spontaneous symmetry breaking. On the other hand, the application of external fields which render the classical system chaotic allows using the double-well to study the interplay between quantum tunnelling and chaos [10]. Moreover, we found that the GK states are related to Schödinger catlike states for high energies, revealing yet another interesting property of this potential.

In section 2 we review the definition of generalized coherent states. Section 3 is devoted to a brief description of the double-well potential. All the results are presented and discussed in section 4 and we conclude in section 5. The classical solution of the system is analysed in the appendix.

2. Gazeau–Klauder coherent states

In this section we present a brief review of the Gazeau–Klauder theory of coherent states for general potentials [3]. Let H be a Hamiltonian with purely discrete nondegenerate (either finite or infinite) spectrum

$$H|n\rangle = \hbar\omega e_n|n\rangle \qquad n \geqslant 0 \tag{2}$$

where the e_n are pure numbers and $e_0 = 0$. From now on we adopt units in which $\hbar = \omega = 1$. The generalized coherent states are then given by

$$|J, \gamma\rangle = \frac{1}{\sqrt{N(J)}} \sum_{n\geqslant 0} \frac{J^{n/2}}{\sqrt{\rho_n}} \mathrm{e}^{-\mathrm{i}e_n\gamma}|n\rangle \tag{3}$$

where $0 \leqslant J \in \mathbb{R}$, $\gamma \in \mathbb{R}$ and ρ_n is an arbitrary function of n with $\rho_0 = 1$. This is a direct generalization of (1), which corresponds to $e_n = n$ and $\rho_n = n!$.

Of course the normalization condition imposes that the series

$$N(J) = \sum_{n\geqslant 0} \frac{J^n}{\rho_n} \tag{4}$$

be convergent for some radius R (which may be infinite). By construction one has the temporal stability property

$$\mathrm{e}^{-\mathrm{i}Ht}|J, \gamma\rangle = |J, \gamma + t\rangle. \tag{5}$$

If the moment problem

$$\int_0^R J^n \frac{W(J)}{N(J)}\,\mathrm{d}J = \rho_n \tag{6}$$

admits a positive solution for $W(J)$, then there exists a resolution of the identity in terms of these states (and in this case they are said to be coherent), in the sense that

$$\lim_{\Gamma\to\infty} \frac{1}{2\Gamma} \int_{-\Gamma}^{\Gamma} \mathrm{d}\gamma \int_0^R \mathrm{d}J\, W(J)|J, \gamma\rangle\langle J, \gamma| = \sum_{n\geqslant 0} |n\rangle\langle n|. \tag{7}$$

The mean value of the Hamiltonian (often called its lower symbol or Q-symbol) in these states is determined by the choice of the function ρ_n. A common choice, which we will adopt in this paper, is to set $\rho_n = e_1 e_2, \ldots, e_n$ for $n > 0$, in which case the variable J can be interpreted as the mean energy:

$$\langle J, \gamma | H | J, \gamma \rangle = J. \tag{8}$$

The coefficients $\langle n|\alpha\rangle$ of the canonical coherent states are known to follow a Poisson distribution. The statistical character of a general state is measured by the Mandel parameter [12]

$$Q = \frac{(\Delta n)^2}{\langle n \rangle} - 1 = \frac{\langle n^2 \rangle - \langle n \rangle^2}{\langle n \rangle} - 1 \tag{9}$$

and a state is said to be Poissonian when $Q = 0$, that is, $(\Delta n)^2 = \langle n \rangle$. The cases $Q < 0$ and $Q > 0$ correspond to so-called sub-Poissonian and super-Poissonian states, respectively (sub-Poissonian statistics is considered a fingerprint of the quantum nature of a state [13]). This parameter gives an estimate of how many states $|n\rangle$ effectively contribute to the superposition (3). In the case of the GK states we have

$$\langle n \rangle = J \frac{\mathrm{d}}{\mathrm{d}J} \ln N(J) \tag{10}$$

and therefore Q is independent of γ and given by

$$Q(J) = J \frac{\mathrm{d}}{\mathrm{d}J} \ln \left[\frac{\mathrm{d}}{\mathrm{d}J} \ln N(J) \right]. \tag{11}$$

It is easy to see that for small J we can approximate this by

$$Q(J) \simeq J \left(\frac{2}{e_2} - \frac{1}{e_1} \right) < 0 \qquad J \ll 1. \tag{12}$$

In what follows we construct GK states for the one-dimensional double-well potential, a system which does not have an underlying algebraic structure and therefore is not suitable for the constuction of Perelomov coherent states [1].

3. The double-well potential

The stationary Schrödinger equation for this system can be written, with dimensionless units, as

$$\left(\frac{1}{2} \frac{\mathrm{d}^2}{\mathrm{d}x^2} - \frac{\beta}{2} x^2 + x^4 \right) \phi_n(x) = e_n \phi_n(x). \tag{13}$$

The height of the potential barrier is $U = \beta^2/16$. The classical solution for the system is shown in the appendix. The quantum version is not solvable analytically, and in order to obtain the energy levels and stationary states we write the Hamiltonian matrix in an appropriate Fourier basis and diagonalize it numerically, using typically a few hundred elements.

In figure 1 we show the first four energy levels (the potential has been shifted so that $e_0 = 0$) and the corresponding eigenfunctions, both for the quartic potential, $\beta = 0$, and for $\beta = 10$. Note that the ground state and the first excited one are almost degenerate in the second case. For high values of β the states below the barrier tend to appear in doublets, and the corresponding eigenstates come in even–odd pairs. This can already be noted in figure 1(b).

We now consider the states defined in (3) and investigate their physical properties. Since the energy levels e_n in this case grow faster than n, the series (4) will be convergent for all J. The corresponding moment problem (6), however, cannot be easily solved and, therefore,

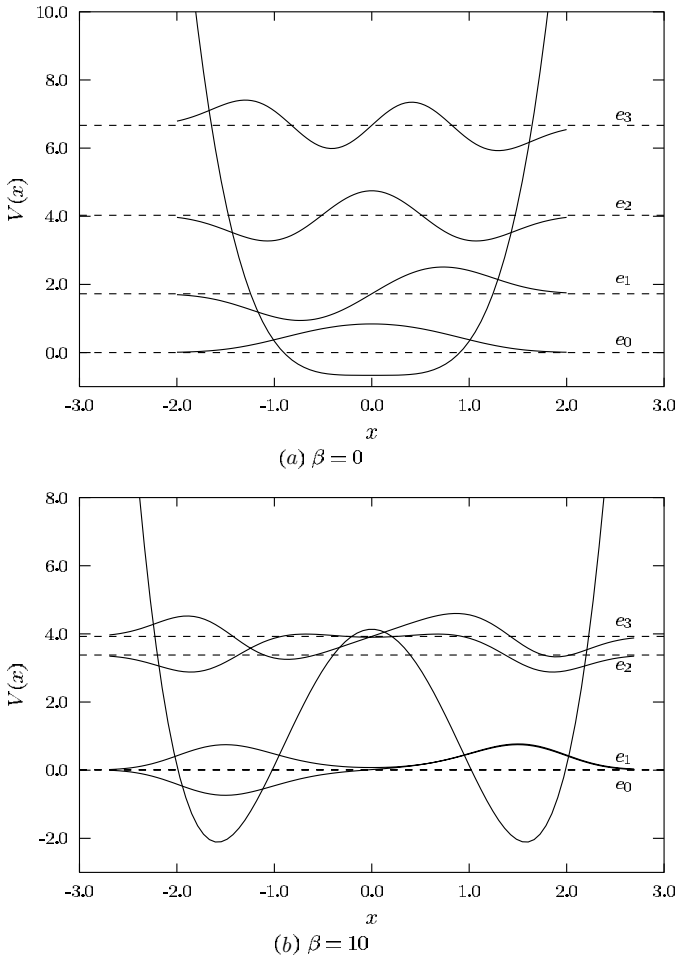

Figure 1. The potential (solid lines) and the first energy levels (dashed lines) for $\beta = 0$ and $\beta = 10$. The energy levels serve as x axes for the corresponding wavefunctions.

the (over-)completeness of this family is still a conjecture. Since J corresponds to the energy measured from the ground state, for $\beta > 0$ there will be a critical value J_c, which equals the height of the barrier, $J_c = U - e_0$, where the classical system is singular.

4. Generalized coherent states

Figure 2 shows the probability density $|\langle x|J, \gamma\rangle|^2$ for a GK state with $\beta = 20$, which gives $J_c \simeq 21.9$. We use $J = 25$, which is close to the potential barrier. Figures 2(a) and (b) correspond to $t = 0$ and $t = T/4$, where T is the classical period of a particle of energy $J - e_0$. We see that an initially localized peak evolves to an intricate distribution, in contrast to the canonical coherent states, reflecting the anharmonicity of the potential. In order to explore the physical properties of these states, we analyse quantities such as their statistical nature, temporal evolution of $\Delta\hat{X}\Delta\hat{P}$, Wigner functions and autocorrelation.

We begin by considering the Mandel parameter, figure 3, and note that the GK states can display all possible behaviour. One can see that $Q(J)$ is always negative for small J, and

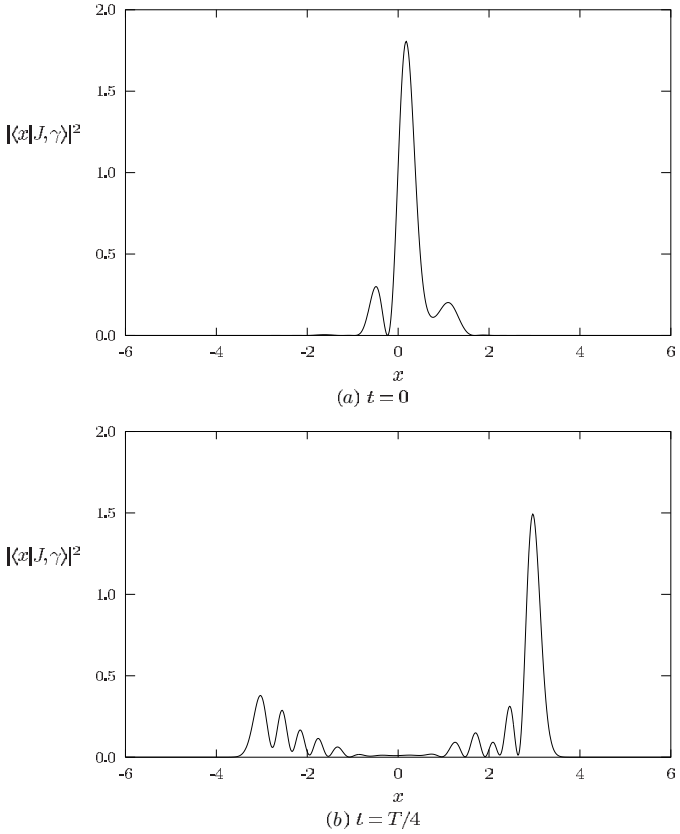

Figure 2. The probability density $|\langle x|J,\gamma\rangle|^2$ associated with a Gazeau–Klauder state for $\beta = 20$ and $J = 25$, for two different values of $\gamma = t$.

that $Q(0) = 0$ for any β, in agreement with (12). Indeed, when $\beta > 0$ the low energy states tend to form doublets and the energy of the first excited state becomes very low. In this case equation (12) can be further approximated by $Q(J) = -J/e_1$. As a result, the Mandel parameter goes from 0 to -1 in a very short J interval, as we see in figure 3(b).

Furthermore, one can see that for high values of β the GK state with $J = e_1$ involves essentially only the first two eigenstates and can be approximated by

$$|J = e_1, \gamma\rangle \simeq \frac{|0\rangle + \mathrm{e}^{\mathrm{i}e_1\gamma}|1\rangle}{\sqrt{2}} \tag{14}$$

which for $\gamma = 0$ is a state localized at one side of the well. As γ evolves to $2\pi/e_1$ the state becomes $(|0\rangle - |1\rangle)/\sqrt{2}$, which is localized at the opposite side. Therefore the particle keeps tunnelling back and forth with an extremely small frequency, proportional to e_1. As J is increased, other basis states become important to the GK superposition, and this simple behaviour disappears. Note that the Mandel parameter for the state (14) can be obtained analytically and is equal to -1.

The Gazeau–Klauder states for the double-well potential are therefore sub-Poissonian for all J if β is less than a critical value β_c, a fingerprint of their non-classicality. When $\beta > \beta_c$, on the other hand, they can become super-Poissonian for a finite range of J, as is clear

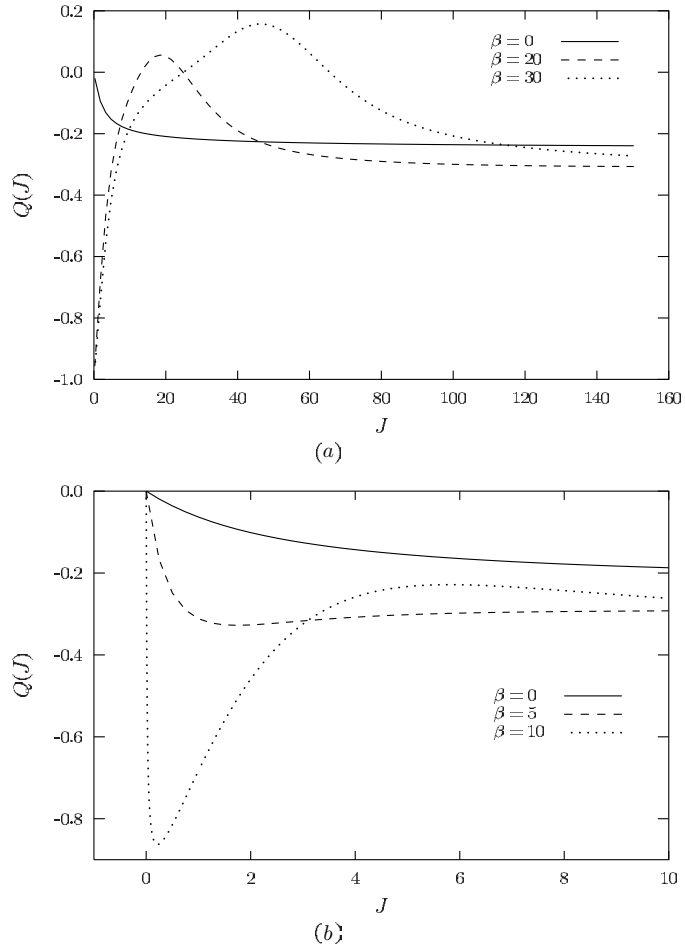

Figure 3. The Mandel parameter can be negative, zero or positive, depending on β and J. In (b) we see only the small-J region. Note that $Q(0) = 0$ for all β.

from figure 3(a). This flexibility is in contrast with the harmonic oscillator case, where the coherent state is always Poissonian (while the squeezed states [15] can display all types of statistics).

Another physical quantity of interest is the time dependence of the dispersion $\Delta\hat{X}\,\Delta\hat{P}$, which must always be bigger than or equal to $\hbar/2$ and that has exactly this value for the canonical coherent state (1). Minimum-uncertainty states were defined for general potentials in a series of papers [16], where the authors discuss the conditions for this property to be realized. An analysis of the double-well along these lines was presented recently [17]. Coherent states derived from Lie algebras, usually called Perelomov coherent states [1], are also known to saturate a generalized uncertainty relation under certain circunstances [18].

We can see in figure 4 the dispersion for the GK states with $J = 1$, measured in units of $\hbar$, both for $\beta = 0$ and $\beta = 10$. Although in the first case the dispersion sometimes comes quite close to the minimum value of $\frac{1}{2}$, we see that the GK states are not minimum-uncertainty states. This does not come as a surprise, since the double-well potential lacks an exact

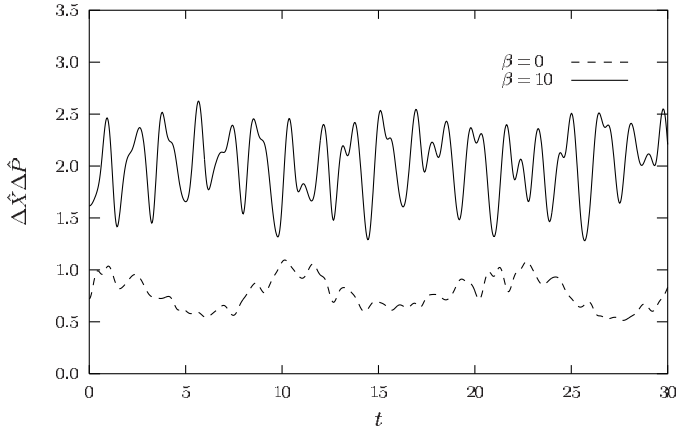

Figure 4. The dispersion $\Delta\hat{X}\Delta\hat{P}$ (in units of $\hbar$) for $J = 1$ as a function of time. The GK states are not of minimum uncertainty.

algebraic formulation. Note also that as β increases so does the average dispersion, and the GK states become more and more different from minimum-uncertainty states.

The double-well potential has recently been considered by one of us (MN) from the point of view of quantum distribution functions [19], namely the Wigner and Husimi functions, but only the stationary states were treated there. We present in figure 5 the Wigner functions $W(x, p)$ associated with the GK states with $J = 1, \gamma = 0$, again for $\beta = 0$ and $\beta = 10$. We see that this function can display quite a complicated structure—besides being even in p, it has no symmetries—and is negative in some portions of the phase space, a signature of the non-classicality of the corresponding quantum state. The Wigner function is not localized around any particular curve, even for the pure quartic oscillator, in contrast to the case of the stationary states. Of course when $J = 0$ the GK state reduces to the ground state, and the corresponding Wigner functions have been analysed in [19].

In figure 6(a) we show the probability density for the GK state at $t = 0$ for a high energy regime, $J = 500$. The value of β is clearly irrelevant in this case. This non-local state with several maxima consists of a superposition of nearly 70 stationary states around a mean number $\langle n\rangle \approx 80$. A few moments later (figure 6(b)), however, one can see the appearance of two minimum-uncertainty packets centred symmetrically around the origin, indicating that it should be possible to find a simple analytical form for the GK state in the asymptotic limit. In fact, in this regime the behaviour of the GK state can be unexpectedly well described by the expression

$$\langle x|J, t\rangle \simeq \frac{\mathrm{e}^{\mathrm{i}\theta(x,t)}}{\mathcal{N}}[\mathrm{e}^{\mathrm{i}\pi/4}\Psi_\alpha(x, t) + \mathrm{e}^{-\mathrm{i}\pi/4}\Psi_{-\alpha}(x, t)] \tag{15}$$

where $\mathcal{N}$ is a normalization constant and $\Psi_\alpha(x, t)$ is the canonical coherent state (1) in the coordinate representation

$$\Psi_\alpha(x, t) = (\pi\sigma(t))^{-1/4}\exp\left\{-\frac{(x - x_{cl}(t))^2}{2\sigma(t)} + \mathrm{i}p_{cl}(t)x\right\} \tag{16}$$

with $\alpha = x_{cl}(t)/\sqrt{\sigma(t)} + \mathrm{i}\sqrt{\sigma(t)}p_{cl}(t)$. The quantities $x_{cl}(t)$ and $p_{cl}(t)$ are the classical position and momentum for a quartic oscillator (see the appendix) with energy equal to J. The time-dependent mean width $\sigma(t)$ and the gauge-like local phase $\theta(x, t)$ must be chosen properly. The agreement between this expression and the numerical data is generally around

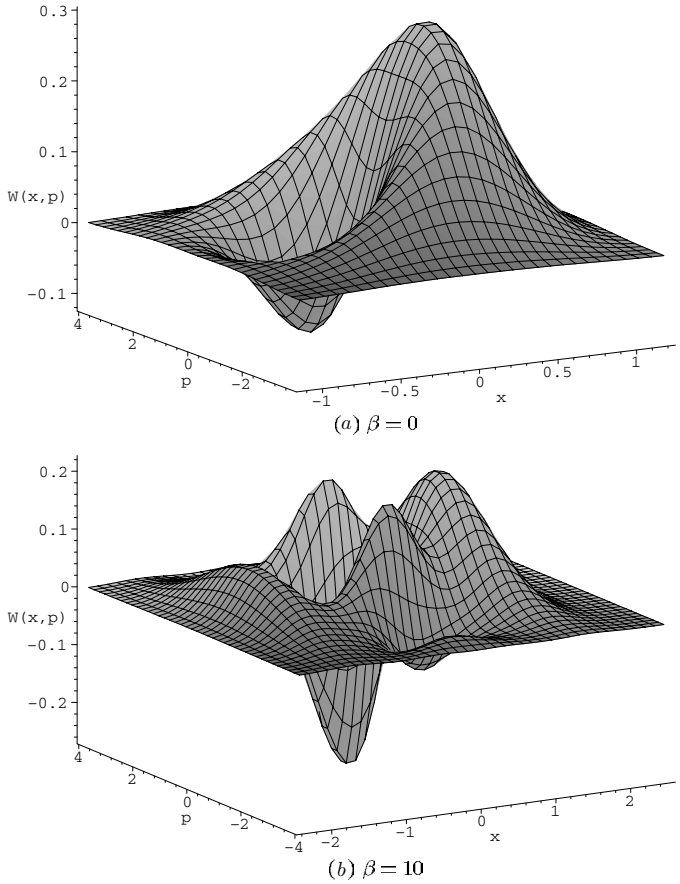

Figure 5. The Wigner functions of the GK states with $J = 1$. They are negative in some regions of phase space, indicating the nonclassical character of the state.

a few per cent, with exceptional agreement (one part per million) when far from the turning points.

The minimum-uncertainty states (16) are famous for being the closest quantum analogue of a classical particle, and are considered to be a macroscopic quantum state when $|\alpha|^2 \gg 1$. Consequently, a superposition of two such states is usually interpreted as a 'macroscopic quantum superposition', an entity that has historically being called a Schrödinger catlike state [20]. Schemes for generation [21], detection [22] and even teleportation [23] of Schrödinger catlike states in QED cavities have been the subject of intense research in the past years. The fact that GK states in a x^4-anharmonic potential are of this kind should be remarked.

In figure 6(c) the Gaussians are at the classical turning points, and the half-period interference is shown in figure 6(d). This wavefunction is orthogonal to the initial one. The Gaussians are again at the turning points in figure 6(e), where we can see the appearance of the small irregularities responsible for the largest deviation between the analytical and numerical solutions. Finally we show in figure 6(f) the probability density after a classical period. It is in phase with the initial state and their overlap is of the order of 60%.

The reconstruction properties of the GK states during time evolution can be analysed by calculating their autocorrelation, $\mathcal{A}(t) = |\langle J, 0|J, t\rangle|^2$, as a function of the excitation energy J and time. The typical low-energy behaviour is shown in figure 7 for $\beta = 10$, which

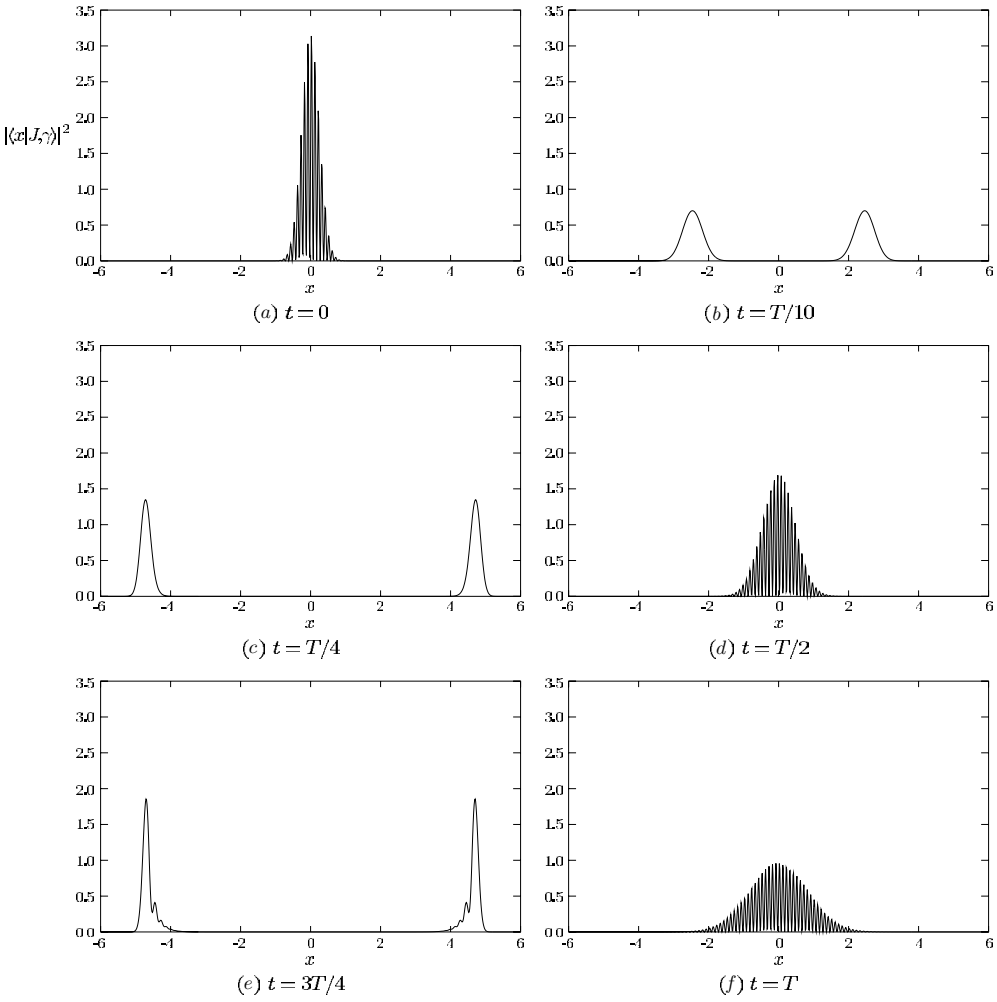

Figure 6. The probability density for the GK state with $J = 500$, at different fractions of the classical period. We see the coherent superposition of two minimum-uncertainty states.

gives $J_c \simeq 4.14$. Each of the several maxima corresponds to a best local reconstruction of the initial state, and we denote the position of the nth maximum by T_n. The intensity of the peak, which corresponds to the fidelity of the reconstruction, is denoted I_n. Figure 7(a) shows an excitation energy of $J = 1$, well below the threshold. The first peak, at $T_1 \simeq 1.8$, shows an almost complete reconstruction of the initial state, with $I_1 \simeq 0.95$, and is followed by two successive maxima with decreasing accuracy of reproduction. After this point the tendency of the initial image to deteriorate is reversed and we see that the two following maxima have increasing intensities. All these first peaks occur, to a good approximation, at multiples of T_1 and therefore the autocorrelation function is quasi-periodic in the short-time scale. Let us denote this 'quantum quasi-period' by τ. A global maximum ($I_1 \simeq 0.99$) is reached around $T_r = 11.3$, and we see that two time scales characterize the behaviour of the system at this point. The first one, τ, is analogous to the classical period, although generally different from it. The second one, the revival time T_r, is roughly an order of magnitude greater and has no classical analogue. Other time scales (for example the so-called super-revival

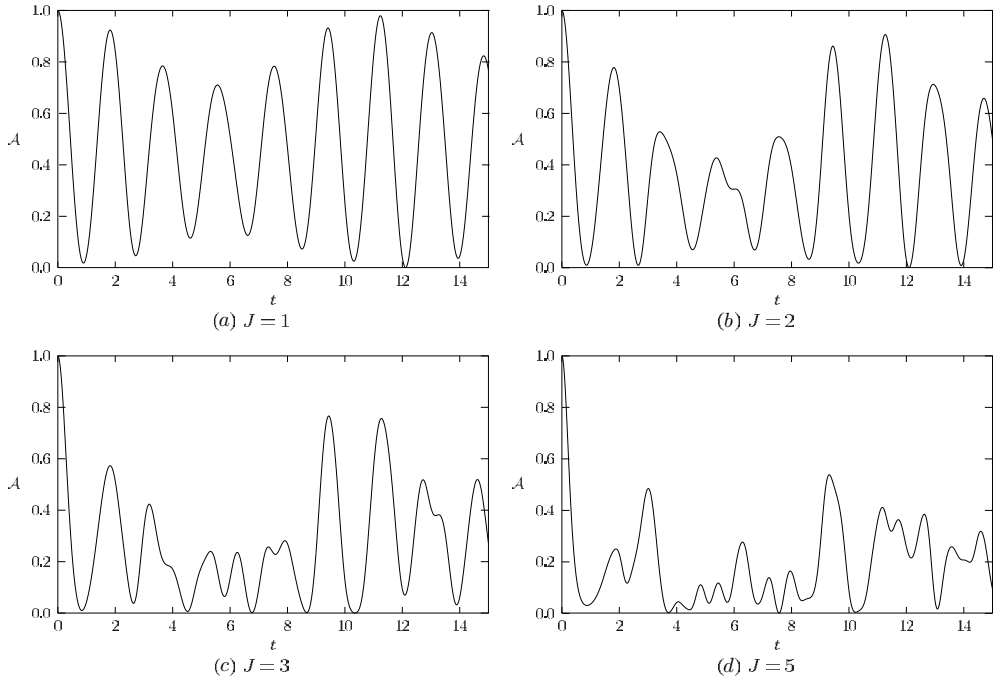

Figure 7. Autocorrelation functions for $\beta = 10$ and different (small) values of J. We can observe the unfolding of the singularities.

time) become important as time increases, but we restrict our attention to the short time evolution.

Figure 7(b) shows the autocorrelation for the same potential but with twice the excitation energy, $J = 2$. The positions of the maxima change moderately but the behaviour of the third peak indicates a process that is central to understanding the dynamics of the GK states under changes in energy: the unfolding of singularities (maxima). We see a side singularity being created close to the third peak, which evolves to twin peaks in figure 7(c): an unstable singularity having unfolded into two maxima and one minimum in a well-known process belonging to singularity theory. Figure 7(c) corresponds to a value of J lower than the barrier threshold ($J = 3$) and figure 7(d) shows the autocorrelation shortly after the crossing of the barrier ($J = 5$). The position of the first maximum, which corresponds to the classical period when the parameters (J, β) are in a particular region, is not strongly affected by the barrier. The same conclusion is valid for the position of the revival time. In both cases the intensities I_τ and I_r rapidly decrease as J increases and crosses the barrier: the singularity position is qualitatively invariant but not its intensity. In particular the revival time becomes poorly characterized as J becomes large (it is already no longer a global maxima in figure 7(d)).

In figure 8 we show some graphics of $\mathcal{A}(t)$ for higher values of J. Let us focus our attention on the fourth peak. It is poorly resolved in the first figure, but as J increases we see the singularities involving the main maximum being suppressed. This is confirmed in figures 8(c) and (d). In the last one the peak is, within the resolution of the figure, smooth. The last figure corresponds to $J = 500$, and is related to the evolution of the catlike state (15). The partial reconstructions occur at multiples of the classical period, but their intensity is progressively weakened due to the time-dependence of the parameter $\sigma(t)$. We must note that the high-energy regularity is different from the low-energy one, as we can see by comparing

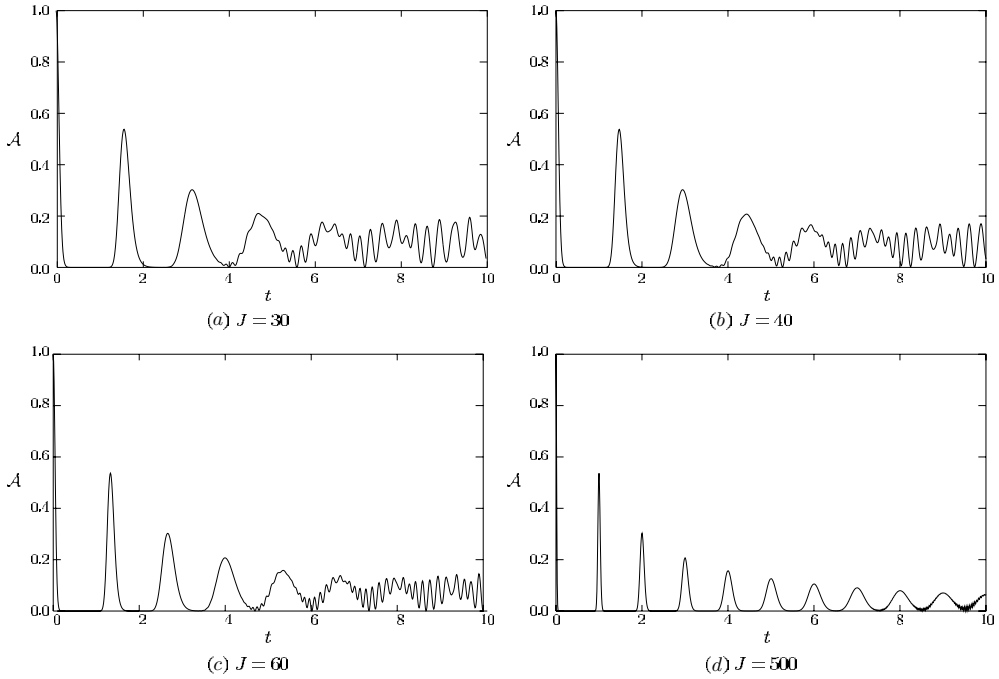

Figure 8. Autocorrelation functions for some higher values of J. We observe the folding of the singularities.

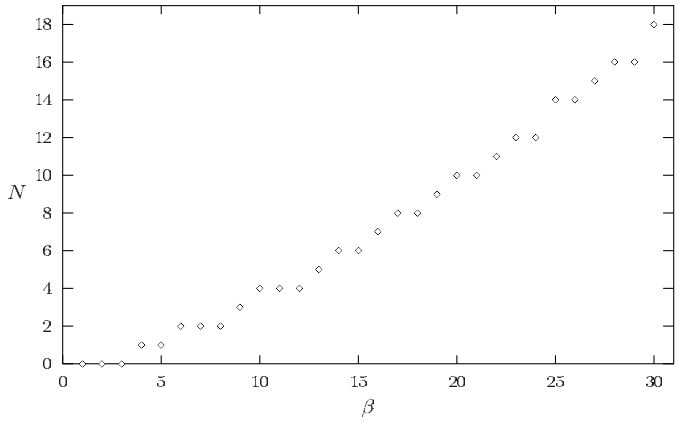

Figure 9. Number of stationary states below the barrier as a function of β.

figures 7(a) and 8(d): another kind of order is reached as the energy is increased. The folding/unfolding of the singularities is the route between the two distinct regimes.

We calculated the autocorrelation for $\beta = 20$ in order to investigate the β-dependence of the low-energy quasi-period τ. We found that in this case τ is indeed the classical period, in contrast to the $\beta = 10$ case. This is explained by the number of stationary states below the barrier in each case. In figure 9 we plot this quantity as a function of β. The relation is approximately linear and we see that there are not 'enough' states in the $\beta = 10$ case for the system to behave 'quasi-classicaly' below the barrier. On the other hand, one will always find

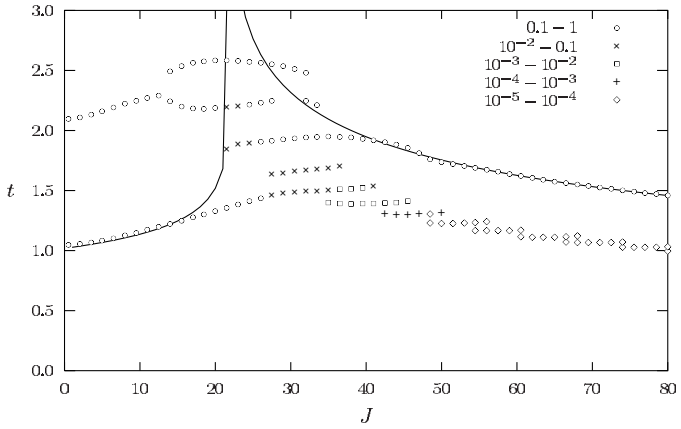

Figure 10. First peaks of the autocorrelation function. Different symbols denote different intensities, and the solid line is the classical period. Note the perfect agreement between the highest peak and the classical period when J is far from the barrier height.

the classical period to be the relevant time scale for sufficently high energy, as we saw in the preceding paragraph.

Finally, we plot in figure 10 the position of the first peaks for $\beta = 20$, as a function of J, together with the corresponding classical period of oscillation, T_{cl}, which is the solid line. Different symbols denote different intensities of reconstruction. It is clear that τ corresponds to T_{cl} when J is very small compared to the barrier. As this threshold is crossed the classical period diverges, but the position of the first peak is not strongly affected. Its intensity, however, is progressively decreased until it practically disappears. A typical bifurcation pattern appears in the position of the second peak around $J = 12$, exhibiting the unfolding of the singularity. Before this branching point the initial state is partially reproduced at T_{cl} and $2T_{cl}$, and immediately after this point two reproducing maxima for the image are created in a short time interval, one of them being dominant. They are both practically unaffected by the crossing of the barrier, but do not survive to the high-energy region. The topological structure of the singularities is more robust and the classical period is part of this structure.

5. Conclusions

We have obtained generalized coherent states for the one-dimensional double-well. These states are not minimum-uncertainty states, and can be either sub-Poissonian or super-Poissonian, depending on the height of the potential barrier and the mean energy. The relation between the low and high energy regimes was considered in terms of the folding and unfolding of the singularities in the autocorrelation function. For high energies these states can be considered Schrödinger catlike states, since they consist of a coherent superposition of two minimum-uncertainty Gaussians.

Acknowledgments

One of us (MN) acknowledges interesting discussions with J P Gazeau and J R Klauder. This work was supported by FAPESP (Fundação de Amparo à Pesquisa do Estado de São Paulo).

Appendix. The classical double-well potential

Let

$$\varepsilon = \frac{1}{2}\left(\frac{\mathrm{d}x}{\mathrm{d}t}\right)^2 - \frac{\beta}{2}x^2 + x^4 \tag{A.1}$$

be the energy of the system in dimensionless units. Note that the pure quartic oscillator corresponds to the value $\beta = 0$. Negative values of ε correspond to 'confined'—below the barrier—movement. We can rewrite (A.1) as

$$\frac{\mathrm{d}x}{\mathrm{d}t} = \sqrt{2\left[\lambda^2 - \left(x^2 - x_0^2\right)^2\right]} \tag{A.2}$$

where

$$x_0^2 = \frac{\beta}{4} \qquad \lambda = |\sqrt{\varepsilon + U}| \qquad U = \frac{\beta^2}{16}. \tag{A.3}$$

Note that U is the barrier height and x_0 are the points corresponding to the minimum of the potential. The turning points are $\pm\sqrt{x_0^2 \pm \lambda}$.

If $\varepsilon > 0$ we can define

$$a^2 = \lambda - x_0^2 \qquad b^2 = \lambda + x_0^2 \tag{A.4}$$

and integrate by quadrature

$$t + t_0 = \int_0^x \frac{\mathrm{d}y}{\sqrt{2(a^2 + y^2)(b^2 - y^2)}} = \frac{1}{\sqrt{2(a^2 + b^2)}}\,\mathrm{sd}^{-1}\left(\frac{x\sqrt{(a^2 + b^2)}}{ab}, \sqrt{\frac{b^2}{a^2 + b^2}}\right) \tag{A.5}$$

to get the solution

$$x(t) = \sqrt{\frac{\varepsilon}{2\lambda}}\,\mathrm{sd}\left(2\sqrt{\lambda}(t + t_0), \sqrt{\frac{\lambda + x_0^2}{2\lambda}}\right) \tag{A.6}$$

where sd is a Jacobi function.

Since the complete elliptic integral of the first kind $K(\kappa)$ is a quarter of the period of the Jacobi $\mathrm{sd}(u, \kappa)$ function, we have the period of the movement as a function of the energy:

$$T_{\varepsilon>0} = \frac{2}{\sqrt{\lambda}}K(\kappa) \tag{A.7}$$

where

$$\kappa = \sqrt{\frac{\lambda + x_0^2}{2\lambda}}. \tag{A.8}$$

The relation between the action variable

$$S_{\varepsilon>0} = 4\int_0^{T/4}\left(\frac{\mathrm{d}x}{\mathrm{d}t}\right)^2 \mathrm{d}t = \frac{4\epsilon}{\sqrt{\lambda}}\int_0^{K(\kappa)} cd^2(u, \kappa)nd^2(u, \kappa)\,\mathrm{d}u \tag{A.9}$$

and the energy can be shown to be [24]:

$$S_{\varepsilon>0} = \frac{8}{3}\sqrt{\lambda}\left[\left(\lambda - x_0^2\right)K(\kappa) + 2x_0^2 E(\kappa)\right] \tag{A.10}$$

where $E(\kappa)$ is the complete elliptic integral of the second kind.

In the confined region $\varepsilon < 0$ an analogous calculation results in

$$x(t) = \sqrt{x_0^2 - \lambda}\,nd\left(\sqrt{2}\sqrt{\lambda + x_0^2}(t + t_0), k^{-1}\right) \tag{A.11}$$

and in this case the period of the motion and the action variable are, respectively

$$T_{\varepsilon<0} = \sqrt{\frac{2}{\lambda + x_0^2}} K(\kappa^{-1}) \tag{A.12}$$

$$S_{\varepsilon<0} = \frac{8}{3\sqrt{2}} \sqrt{\lambda + x_0^2} \left[\left(\lambda - x_0^2\right) K\left(\kappa^{-1}\right) + x_0^2 E(\kappa^{-1}) \right]. \tag{A.13}$$

This system has a singular behaviour for $\varepsilon = 0$, in which case the trajectory is called the separatrix, when the period of the movement goes to infinity and the action variable has a discontinuity. In this case we have the quadrature integral (assuming the particle to be at the turning point in $t = 0$)

$$t = \int_{\sqrt{\beta/2}}^{x} \frac{\mathrm{d}y}{\sqrt{2y^2(\beta/2 - y^2)}} = \frac{1}{\sqrt{\beta}} \ln \left[\frac{\sqrt{\beta} + \sqrt{\beta + 2x^2}}{\sqrt{2}x} \right] \tag{A.14}$$

which gives

$$x(t) = \sqrt{\frac{\beta}{2}} \frac{1}{\cosh(\sqrt{\beta}t)}. \tag{A.15}$$

References

[1] Perelomov A 1986 *Generalized Coherent States and Their Applications* (Berlin: Springer)
[2] Ali S T, Antoine J P and Gazeau J P 2000 *Coherent States, Wavelets and Their Generalizations* (New York: Springer)
[3] Klauder J R 1996 *J. Phys. A: Math. Gen.* **29** L293
Gazeau J P and Klauder J R 1999 *J. Phys. A: Math. Gen.* **32** 123
[4] Antoine J P, Gazeau J P, Monceau P, Klauder J R and Penson K A 2001 *J. Math. Phys.* **42** 2349
[5] El Kinani A H and Daoud M 2001 *Int. J. Mod. Phys.* B **15** 2465
[6] Hollingworth J M, Konstadopoulou A, Chountasis S, Vourdas A and Backhouse N B 2001 *J. Phys. A: Math. Gen.* **34** 9463
[7] El Kinani A H and Daoud M 2002 *J. Math. Phys.* **43** 714
El Kinani A H and Daoud M 2001 *J. Phys. A: Math. Gen.* **34** 5373
[8] Daoud M and El Kinani A H 2002 *J. Phys. A: Math. Gen.* **35** 2639
[9] Novaes M and Gazeau J P 2003 *J. Phys. A: Math. Gen.* **36** 199
[10] Bies W E, Kaplan L and Heller E J 2001 *Phys. Rev.* E **64** 016204
Grifoni M and Hänggi P 1998 *Phys. Rep.* **304** 229
Grossmann F, Dittrich T, Jung P and Hänggi P 1991 *Phys. Rev. Lett.* **67** 516
Bohigas O, Tomsovic S and Ullmo D 1993 *Phys. Rep.* **2** 43
[11] Klauder J R, Penson K A and Sixdeniers J M 2001 *Phys. Rev.* A **64** 013817
Sixdeniers J M, Penson K A and Solomon A I 1999 *J. Phys. A: Math. Gen.* **32** 7543
[12] Mandel L 1979 *Opt. Lett.* **4** 205
[13] Davidovich L 1996 *Rev. Mod. Phys.* **68** 127
[14] Bluhm R, Kostelecky V A and Porter J A 1996 *Am. J. Phys.* **64** 944
[15] Walls D F 1983 *Nature* **306** 141
[16] Nieto M M 1981 *Phys. Rev.* D **23** 927
[17] Nieto M M 2001 *Mod. Phys. Lett.* A **16** 2305
[18] Klauder J R and Skagerstam B-S (ed) 1985 *Coherent States: Applications in Physics and Mathematical Physics* (Singapore: World Scientific)
[19] Novaes M *J. Opt. B: Quantum Semiclass. Opt.* submitted
[20] Schrödinger E 1935 *Naturwissenschaften* **23** 812
[21] Yurke B and Stoler D 1986 *Phys. Rev. Lett.* **57** 13
Gerry C C and Grobe R 1998 *Phys. Rev.* A **57** 2247
[22] Brune M *et al* 1996 *Phys. Rev. Lett.* **77** 4887
[23] Davidovich L, Zagury N, Brune M, Raimond J M and Haroche S 1994 *Phys. Rev.* A **50** R895
Moussa M H Y 1997 *Phys. Rev.* A **55** R3287
de Almeida N G, Napolitano R and Moussa M H Y 1999 *Phys. Rev.* A **62** 010 101
[24] Byrd P F and Friedman M D 1971 *Handbook of Elliptic Integrals for Engineers and Scientists* (New York: Springer) p 213